Available online at www.sciencedirect.com
ScienceDirect
Thin Solid Films 515 (2007) 5606–5610
www.elsevier.com/locate/tsf

Energy-dispersive X-ray reflectivity and GID for real-time growth studies of pentacene thin films

S. Kowarik [a,b,*], A. Gerlach [a,b], W. Leitenberger [c], J. Hu [a], G. Witte [d], C. Wöll [d], U. Pietsch [e], F. Schreiber [b]

[a] Oxford University, Physical and Theoretical Chemistry, Oxford OX1 3QZ, UK
[b] Universität Tübingen, Institut für Angewandte Physik, 72076 Tübingen, Germany
[c] Universität Potsdam, Institut für Physik, 14469 Potsdam, Germany
[d] Ruhr-Universität Bochum, 44780 Bochum, Germany
[e] Universität Siegen, 57068 Siegen, Germany

Available online 22 January 2007

Abstract

We use energy-dispersive X-ray reflectivity and grazing incidence diffraction (GID) to follow the growth of the crystalline organic semiconductor pentacene on silicon oxide *in-situ* and in *real-time*. The technique allows for monitoring Bragg reflections and measuring X-ray growth oscillations with a time resolution of 1 min in a wide q-range in reciprocal space extending over 0.25–0.80 $Å^{-1}$, i.e. sampling a large number of Fourier components simultaneously. A quantitative analysis of growth oscillations at several q-points yields the evolution of the surface roughness, showing a marked transition from layer-by-layer growth to strong roughening after four monolayers of pentacene have been deposited.
© 2006 Elsevier B.V. All rights reserved.

Keywords: X-ray diffraction; X-ray reflectivity; Organic semiconductors; Real-time monitoring

1. Introduction

A detailed understanding of organic molecular beam deposition is of great interest in technical applications as well as in growth theory as an important branch of statistical physics [1]. There have been strong efforts to develop a theoretical description of growth phenomena, in particular using scaling laws relating the surface roughness to lateral and vertical length scales (film thickness) [2,3]. The growth of *organic* systems such as pentacene exhibits important qualitative differences, which are not included in the established approaches. One of the most important differences is related to the orientational degrees of freedom, which imply that the problem is generally anisotropic, and that not only the positional adsorption state of a molecule, but also its orientation must be considered [4–7].

Experimentally, real-time monitoring tools allow for following growth kinetics, including the structural evolution and transient phenomena during growth [8]. For *in-situ* and *real-time* studies various non-invasive scattering techniques have been employed including RHEED [9], He-scattering [10], and X-ray scattering [8,11,12], but also optical techniques such as reflection anisotropy spectroscopy [13].

In this work we use energy-dispersive X-ray reflectivity and grazing incidence diffraction (GID), which has the advantage of high spatial resolution and can be analysed in most cases by a simple single scattering (kinematic) theory. While X-ray growth oscillations at one point in reciprocal space have been routinely monitored in growth studies [11,12,14–16], the energy-dispersive technique offers the advantage of simultaneously measuring a wide q-range, i.e. a large number of Fourier components are sampled. This allows for a more reliable and detailed analysis of structural and morphological changes during growth.

Here we follow the growth of the organic semiconductor pentacene, a model system for organic molecular beam deposition and also a promising material for organic field effect transistors [17]. We determine the out-of-plane structure of pentacene in real-time during growth, demonstrating the potential of the technique. We present a quantitative analysis of real-time growth oscillations not only at the anti-Bragg point,

* Corresponding author. Universität Tübingen, Institut für Angewandte Physik, 72076 Tübingen, Germany. Tel.: +49 7071 2976389; fax: +49 7071 29 5110.
E-mail address: Stefan.Kowarik@uni-tuebingen.de (S. Kowarik).

0040-6090/$ - see front matter © 2006 Elsevier B.V. All rights reserved.
doi:10.1016/j.tsf.2006.12.020

but in a wide q-range, which provides information about the dynamic evolution of the surface roughness with good resolution. We demonstrate that pentacene growth exhibits a marked transition from layer-by-layer growth to strong roughening after a thickness of about four pentacene (mono-) layers.

2. Experimental

The real-time reflectometry during pentacene deposition has been performed at the BESSY II synchrotron source (EDR-beamline) using an energy-dispersive reflectivity setup [18]. As compared to a fixed-energy angular-dispersive reflectometer the energy-dispersive technique works at a fixed angle, so that the sample/UHV chamber does not have to be scanned in angle during deposition, simplifying the setup. The energy-dispersive technique allows acquiring growth oscillations not only at a single point in q-space, but in a wide q-range simultaneously. The energy-dispersive beamline uses a white incident X-ray beam from a bending magnet with a usable energy range of 6–18 keV. Different energies which correspond to different momentum transfers q are separated in an energy-dispersive Roentec detector with a resolution of $\Delta E/E<2\cdot 10^{-2}$. This translates into an out-of-plane resolution of 0.01 Å^{-1} and an in-plane resolution in grazing incidence diffraction of 0.05 Å^{-1} under the experimental conditions employed in this study.

The time resolution for acquisition of an out-of-plane q-range between 0.25 and 0.8 Å^{-1} as used in this study are ~60 s to obtain sufficient counting statistics. This experimental time resolution is suited to study intrinsically slow growth processes, for the present study the acquisition time corresponds to 1/8 of the period of anti-Bragg oscillations. The time resolution is limited not by the flux at the beamline, but by the maximum count rate of the detector. The growth of pentacene ($C_{22}H_{14}$, purchased from Fluka, see Fig. 1, inset) thin films was performed by molecular beam deposition in a portable UHV chamber similar to the one described in Ref. [19] at a base pressure of $\sim 1\cdot 10^{-9}$ mbar. The UHV chamber can be mounted onto an X-ray diffractometer and is equipped with an effusion cell, a thickness monitor, and a Be-window transparent for X-rays, so that *in-situ* and *real-time* experiments are possible. Growth was performed on a silicon wafer with native oxide layer at a temperature of 50 °C with a rate of ~3.5 Å/min, that is ~0.2 monolayers/min. All measurements (real-time and post growth experiments) have been performed *in-situ*, i.e. without breaking the vacuum.

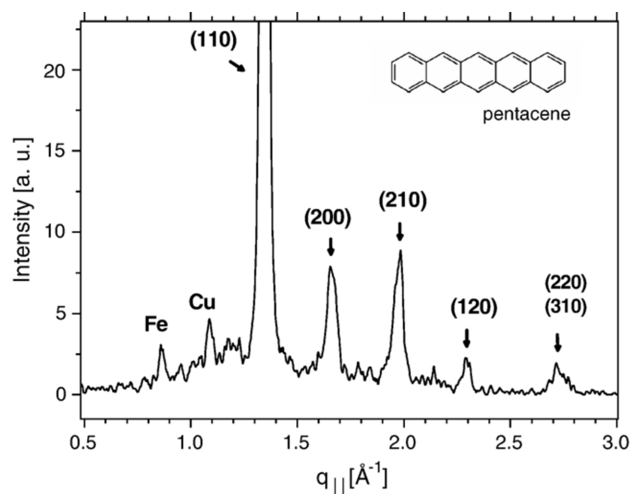

Fig. 1. Energy-dispersive grazing incidence diffraction (angle of incidence $\alpha_i = 0.08°$) for a pentacene film of 14 monolayer thickness. In-plane reflections of pentacene are indexed following Ref. [20].

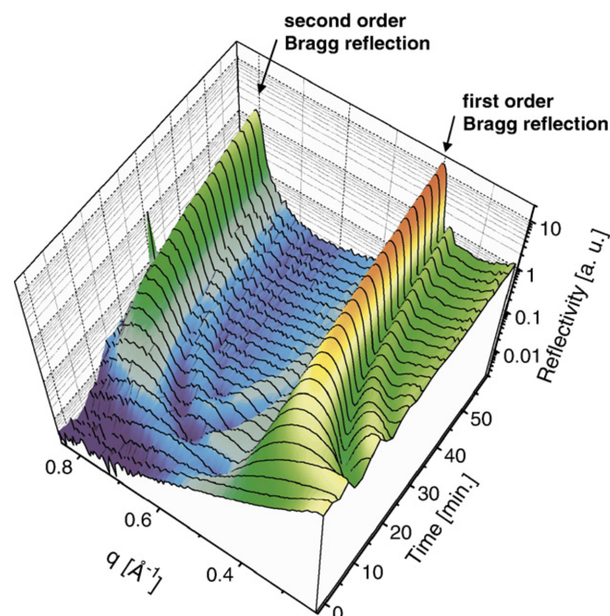

Fig. 2. Evolution of the specular X-ray reflectivity during pentacene growth on oxidized silicon wafers, showing the growth of the first and second order Bragg reflection, as well as narrowing of Laue-oscillations with increasing film thickness (time).

3. Results

Using energy-dispersive grazing incidence diffraction (GID) the in-plane structure (parallel to the substrate) of pentacene films was determined after growth, while the out-of-plane structure (perpendicular to the substrate) was probed by specular X-ray reflectivity in *real-time* during growth.

Fig. 1 shows the in-plane Bragg reflections measured in GID. In the GID data fluorescence lines of iron and copper are also present, but they can be clearly distinguished from Bragg reflections, as they are at fixed energies and do not show any angular dependency when moving the detector. The peak positions in Fig. 1 are consistent with a rectangular unit cell with a herringbone packing motive of pentacene [20]. We extract values of the in-plane unit cell of $a=7.6\pm 0.2$ Å and $b=5.9\pm 0.2$ Å, showing that the thin film phase and not the bulk phase (bulk phase: $a=7.90$ Å, $b=6.06$ Å [20]) grows for the substrate temperature and growth rates used [21].

To follow the evolution of the out-of-plane structure (perpendicular to the substrate) the specular reflectivity was acquired in a range comprising the first and second order Bragg reflections of pentacene as shown in Fig. 2. From the positions

of the Bragg reflections the lattice spacing of the pentacene crystal can be extracted to be 15.4±0.1 Å, confirming that the thin film phase grows. During growth the real-time data-set of Fig. 2 reveals an increasing intensity, narrowing, and shifting of the Bragg reflection. While a decrease in the out-of-plane lattice constant (e.g. by standing upright molecules tilting down in higher layers) has been reported in Ref. [22] the shifting of the maximum of the diffraction feature from ~0.340 $Å^{-1}$ to 0.409 $Å^{-1}$ with increasing film thickness (Fig. 2) does not directly correspond to a similarly substantial change in the lattice constant. Instead, as simulations show [23] interference between substrate and film scattering leads to a change in the shape of the Bragg reflection and thereby a shift of the maximum. Explaining the shift solely by a changing lattice constant an unrealistically large value of more than 18 Å (larger than the ~16.5 Å of the long axis of the pentacene molecule) would have to be assumed for the first monolayers, showing that the major contribution to the shift is due to substrate interference.

From the narrowing of the Bragg reflections and Laue-fringes information about the coherent film thickness, which in this case is equal to the total film thickness, can be extracted. While the data of Fig. 2 can be analysed at fixed times during growth for example by the Parratt formalism, here we focus on the quantitative analysis of growth oscillations, i.e. cuts through Fig. 2 at fixed values of q as a function of time.

On a qualitative level information can be extracted directly from the growth oscillations, such as from the 3/2-anti-Bragg oscillations (see Fig. 3). From the period of two monolayers per oscillation the number of layers deposited can be extracted, while from the damping of the oscillation envelope a deviation from layer-by-layer growth after four monolayers can be inferred. Within the time resolution of 1/8 of the oscillation period (i.e. 1/4 of a monolayer) there is no delay in the oscillations after opening the effusion cell shutter, and the oscillation period does not change, showing that the standing up phase nucleates immediately and also no significant variations in the sticking coefficient occur during deposition, in contrast to pentacene on silicon (without oxide) [24].

For a more quantitative analysis of the real-time growth oscillation we employed kinematical (i.e. single scattering) scattering theory [25] to describe growth oscillations at several q-values as shown in Fig. 3 for 2/3, 3/4, 4/5, 5/6, and 3/2 q_{Bragg}. In kinematic approximation, the total reflected intensity can be calculated by adding (complex) scattering amplitudes for the substrate and every layer of the pentacene film with the correct phase:

$$I_{\text{reflected}}(t) = |f_{\text{substrate}}(q) \cdot e^{i \cdot \Phi(q)} + f(q) \cdot \sum_n \theta_n(t) \cdot e^{i \cdot n \cdot q \cdot d}|^2. \quad (1)$$

$f_{\text{substrate}}(q)$, $f(q)$ substrate form factor and atomic/molecular form factor in the film;
$\Phi(q)$ phase between substrate and molecular scattering;
n layer number;
θ_n fractional coverage of the nth-layer (0 — zero coverage, 1 — filled layer);
q X-ray wavevector transfer upon reflection;
d lattice spacing of the crystalline thin film;

Eq. (1) determines the shape and period of growth oscillations, for example for the anti-Bragg condition $q=1/2 \cdot q_{\text{Bragg}}=\pi/d$ the phase factor in the sum varies between +1 and −1 so that consecutive layers interfere destructively — even monolayers (second, fourth, …layer) exactly cancel the scattering contribution of odd monolayers (first, third, …layer).

In contrast to studies where anti-Bragg oscillations were used to determine the growth kinetics [12,26], energy-dispersive reflectometry allows to measure simultaneously growth oscillations at several q-values allowing for a determination of the layer coverages $\theta_n(t)$ beyond the point where anti-Bragg oscillations are damped out. According to Eq. (1) also for q-values other than the anti-Bragg condition there are growth oscillations with increasing period (three monolayer period for $q=2/3 \cdot q_{\text{Bragg}}$, four monolayers for $q=3/4 \cdot q_{\text{Bragg}}$ … [27]) and, importantly, these growth oscillations contain additional information. While the anti-Bragg oscillations project the $\theta_n(t)$ onto a 'two level system' of odd and even monolayers, 2/3-Bragg oscillations project on a 'three level system' and therefore remove ambiguities between layer coverages such as $\theta_{n=1}(t)$ and $\theta_{n=3}(t)$. For a fit of the growth oscillations in Fig. 3 the unknown parameters $f_{\text{substrate}}(q)$, $f(q)$, and $\Phi(q)$ were calculated from experimental values. Inverting Eq. (1) the three unknown parameters can be obtained from the experimental values for

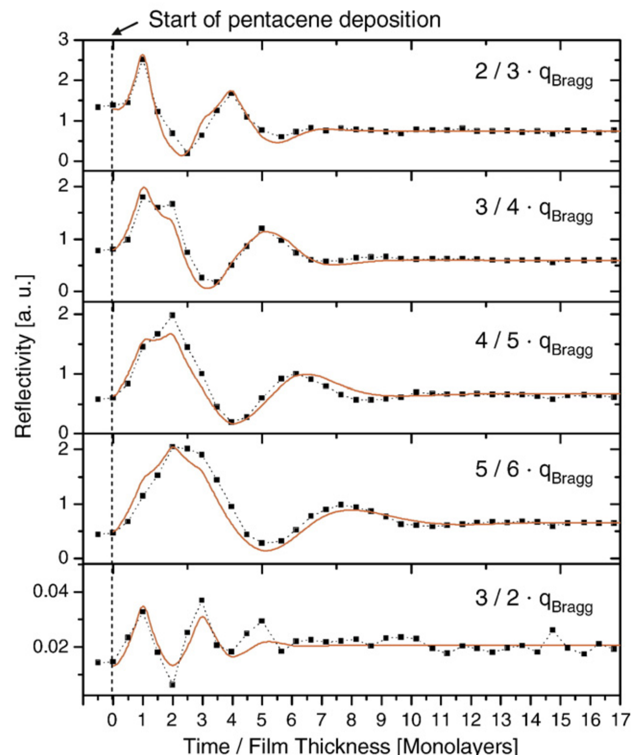

Fig. 3. Growth oscillations for the 2/3-, 3/4- …Bragg condition acquired simultaneously during film growth of pentacene. The solid line is a fit to the data using a diffusive rate equation model (see text).

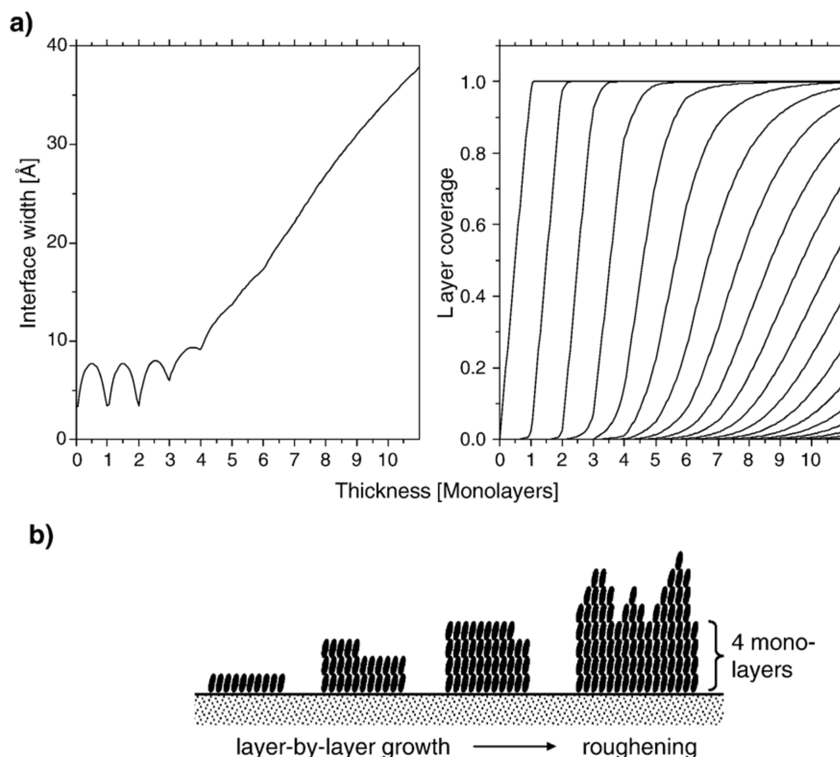

Fig. 4. a) Roughness evolution and layer coverages resulting from a fit to the growth oscillations in Fig. 3. After growth of four monolayers of pentacene the interface width (surface roughness) increases significantly. b) Schematic depicting the transition from layer-by-layer growth to roughening after four monolayers, during growth of the pentacene thin film phase [21].

bare substrate reflectivity, saturation value of the reflectivity, and the reflectivity of one closed monolayer (using the assumption that pentacene starts to grow in a layer-by-layer fashion in the first layer [12]). Finally the time dependence of the $\theta_n(t)$ was modeled with a diffusive rate equation model after reference [28]. The rate constants for interlayer transport entering this model were allowed to decrease for thick films to incorporate effects of an increasing Schwoebel barrier, faster nucleation and/or decreased diffusivity for upper layers.

A simultaneous fit of this model to the experimental growth oscillations [29] is shown in Fig. 3, reproducing the main experimental features like oscillation period and damping of the oscillations. Importantly, the damping for oscillations close to the Bragg condition is weaker than the damping for the anti-Bragg condition, so that the growth dynamics can be followed for longer time than by only observing oscillations at the anti-Bragg condition.

The $\theta_n(t)$ and interface width resulting from the model are shown in Fig. 4. The interface width is a measure for the film roughness and is defined as the standard deviation of the surface from the average film thickness. As can be seen from the interface width and layer coverages $\theta(t)$ in Fig. 4, the pentacene growth exhibits strong roughening after about four monolayers so that the growth oscillations get damped out quickly. While roughness oscillations can be seen for the first four monolayers as expected for layer-by-layer growth there is a marked transition to a rough morphology after four monolayers. While the exact nature of this transition is unknown, the model results indicate a significant drop in interlayer transport. Several factors may contribute to this decreased transport such as faster nucleation and decreased diffusivity, but also an increased Schwoebel barrier may contribute to the roughening.

4. Conclusions

In conclusion we have shown that real-time X-ray reflectivity measurements performed with an energy-dispersive setup are a powerful tool for the characterisation of structure as well as growth dynamics of thin films. Real-time measurements in a wide q-range with a time resolution of 1 min allow for monitoring Bragg reflections and growth oscillations simultaneously. A quantitative analysis of growth oscillations at several q-points gives the evolution of the surface roughness, showing a transition from layer-by-layer growth to roughening after four monolayers of pentacene have been deposited.

Acknowledgements

We gratefully acknowledge experimental help by M. Skoda and financial support by the EPSRC and the DFG.

References

[1] J. Krug, T. Michely, Islands, Mounds and Atoms: Patterns and Processes in Crystal Growth Far From Equilibrium, Springer, Heidelberg, 2004.
[2] A. Pimpinelli, J. Villain, Physics of Crystal Growth, Cambridge University Press, Cambridge, 1998.
[3] J. Krug, Physica A 340 (2004) 647.
[4] F. Schreiber, Phys. Status Solidi, A Appl. Res. 201 (2004) 1037.

[5] W.E. Brütting, Physics of Organic Semiconductors, Wiley-VCH, Berlin, 2005.
[6] A.C. Dürr, F. Schreiber, K.A. Ritley, V. Kruppa, J. Krug, H. Dosch, B. Struth, Phys. Rev. Lett. 90 (2003) 016104.
[7] G. Witte, C. Wöll, J. Mater. Res. 19 (2004) 1889.
[8] S. Kowarik, A. Gerlach, S. Sellner, F. Schreiber, L. Cavalcanti, O. Konovalov, Phys. Rev. Lett. 96 (2006) 125504.
[9] W. Braun, L. Däweritz, K.H. Ploog, Phys. Rev. Lett. 80 (1998) 4935.
[10] S. Söhnchen, S. Lukas, G. Witte, J. Chem. Phys. 121 (2004) 525.
[11] H.H. Teng, P. Fenter, L. Cheng, N.C. Sturchio, Geochim. Cosmochim. Acta 65 (2001) 3459.
[12] A.C. Mayer, R. Ruiz, R.L. Headrick, A. Kazimirov, G.G. Malliaras, Org. Electron. 5 (2004) 257.
[13] J.T. Zettler, K. Haberland, M. Zorn, M. Pristovsek, W. Richter, P. Kurpas, M. Weyers, J. Cryst. Growth 195 (1998) 151.
[14] B. Krause, F. Schreiber, H. Dosch, A. Pimpinelli, O.H. Seeck, Europhys. Lett. 65 (2004) 372.
[15] E. Vlieg, A.W. Denier van der Gon, J.F. van der Veen, J.E. Macdonald, C. Norris, Phys. Rev. Lett. 61 (1988) 2241.
[16] C.L. Nicklin, M.J. Everard, C. Norris, S.L. Bennett, Phys. Rev., B, Condens. Matter Mater. Phys. 70 (2004) 235413/1.
[17] C.D. Dimitrakopoulos, P.R.L. Malenfant, Adv. Mater. (2002) 99.
[18] U. Pietsch, J. Grenzer, T. Geue, F. Neissendorfer, G. Brezsesinski, C. Symietz, H. Möhwald, W. Gudat, Nucl. Instrum. Methods Phys. Res., Sect. A, Accel. Spectrom. Detect. Assoc. Equip. 467–468 (2001) 1077.
[19] K.A. Ritley, B. Krause, F. Schreiber, H. Dosch, Rev. Sci. Instrum. 72 (2001) 1453.
[20] R. Ruiz, A.C. Mayer, G.G. Malliaras, B. Nickel, G. Scoles, A. Kazimirov, H. Kim, R.L. Headrick, Z. Islam, Appl. Phys. Lett. 85 (2004) 4926.
[21] I.P.M. Bouchoms, W.A. Schoonveld, J. Vrijmoeth, T.M. Klapwijk, Synth. Met. 104 (1999) 175.
[22] G. Yoshikawa, T. Miyadera, R. Onoki, K. Ueno, I. Nakai, S. Entani, S. Ikeda, D. Guo, M. Kiguchi, H. Kondoh, Surf. Sci. 600 (2006) 2518.
[23] S. Kowarik, et al., in preparation.
[24] F.J. Meyer zu Heringdorf, M.C. Reuter, R.M. Tromp, Nature 412 (2001) 517.
[25] J. Als-Nielsen, D. McMorrow, Elements of Modern X-ray Physics, Wiley, New York, 2001.
[26] A.C. Mayer, R. Ruiz, H. Zhou, R. Headrick, A. Kazimirov, G.G. Malliaras, Phys. Rev., B 73 (2006) 205307.
[27] E. Weschke, C. Schüβler-Langeheine, R. Meier, G. Kaindl, C. Sutter, D. Abernathy, G. Grübel, Phys. Rev. Lett. 79 (1997) 3954.
[28] P.I. Cohen, G.S. Petrich, P.R. Pukite, G.J. Whaley, A.S. Arrott, Surf. Sci. 216 (1989) 222.
[29] The limited experimental time resolution was accounted for in the simulations.